Drift Orbit and Magnetic Surface Measurements in the Helically Symmetric Experiment

J.N. Talmadge, V. Sakaguchi, F.S.B. Anderson, D.T. Anderson, A. F. Almagri
HSX Plasma Laboratory, University of Wisconsin-Madison, Madison, WI 53706, USA
Email: talmadge@facstaff.wisc.edu

Abstract. HSX is a toroidal quasihelically-symmetric stellarator with negligibly small toroidal curvature. Vacuum magnetic surfaces at 1 kG are measured using low-energy electron beams that strike a fluorescent mesh. The images are recorded with a CCD camera and show no observable evidence of island structures inside the separatrix. The experimental determination of the rotational transform agrees with numerical calculations to within 1%. A simple analytic expression is derived in Boozer coordinates to relate the drift orbits of passing particles to the magnetic field spectrum. This expression is used to analyze images of high-energy electron orbits in HSX, using a neural network to map the lab coordinate system into Boozer coordinates. At very low magnetic field strengths (90 G) where the b_{11} component due to the earth's field is not ignorable, this spectral component and the dominant helical term b_{41} can be experimentally determined. The data does not show the magnitude and direction of the orbit shift that would be expected from the standard toroidal curvature term that exists in other toroidal devices. The results also confirm for the first time that quasihelical stellarators have a large effective transform that is responsible for small drifts of particles off a flux surface.

1. Introduction

The Helically Symmetric Experiment (HSX) is an advanced toroidal stellarator that has been designed to have minimal toroidal curvature and a direction of symmetry in the helical direction with respect to the magnitude of the magnetic field. This form of symmetry, referred to as "quasihelical symmetry", is achieved by careful shaping of the outer flux surface to reduce the toroidal curvature by about a factor of 50 compared to a conventional stellarator with the same aspect ratio. The magnetic field spectrum in the straight field line, Boozer coordinate system is written as

$$B/B_0 = \sum b_{nm} \cos(n\phi - m\theta), \qquad (1)$$

where n is the toroidal mode number and m is the poloidal mode number. The standard configuration in HSX has a single dominant helical term, b_{41} where n = 4 and m = 1.

Neoclassical transport in HSX is similar to that in a tokamak except that HSX has a much higher effective transform given by $\iota_{eff} = n - m\iota$. Since HSX has a transform just above 1, the effective transform is about 3. Theoretically, the very high effective transform is responsible for small drifts of passing particles from a flux surface, small banana widths for trapped particles, very low neoclassical transport for a stellarator, small plasma currents and a small Shafranov shift at finite beta. In this paper, a low-energy electron beam and a fluorescent mesh are used to map the vacuum magnetic surfaces. At higher energy and lower magnetic fields, we demonstrate how the deviation of passing particle orbits from a flux surface can be used to obtain the $m \neq 0$ terms of the magnetic field spectrum.

2. Vacuum Flux Surfaces

Vacuum magnetic surfaces in HSX are measured using a low-energy (20-50 eV) electron beam in a steady-state magnetic field of 1 kG. At this energy and magnetic field, the deviation of the electron orbits from a flux surface is less than 0.1 mm. A copper-wire mesh, with 3 mm grid spacing and a fluorescent coating, is located almost 180^0 from the electron

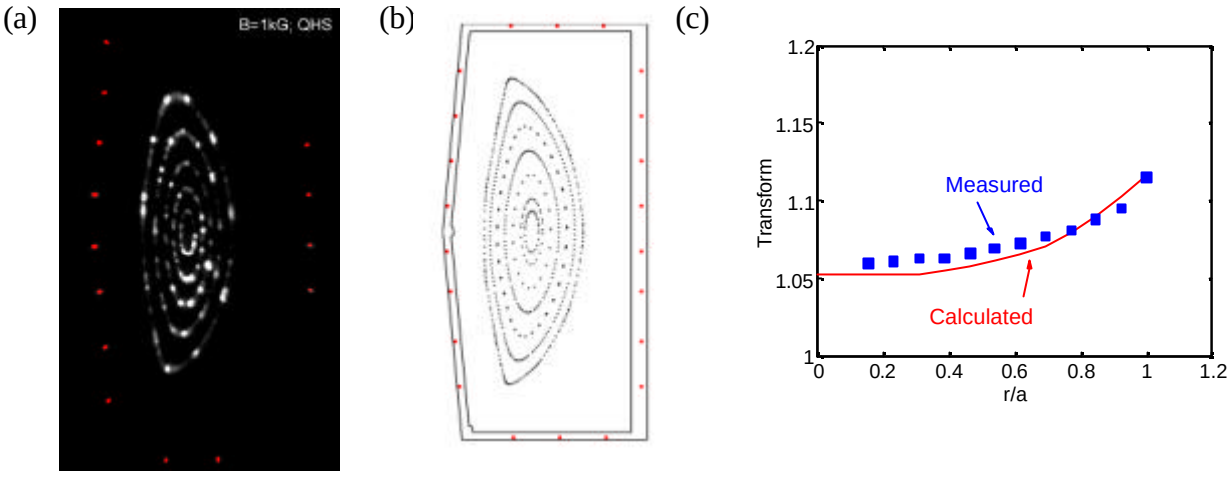

FIG. 1. (a) Measured magnetic surfaces using an electron gun and fluorescent mesh, (b) Calculated flux surfaces, (c) Rotational transform as a function of normalized radius.

gun. Along the frame surrounding the mesh are 22 light-emitting diodes that are used to provide reference points for the images produced when the electrons strike the mesh. A high sensitivity CCD camera records the image, which is then digitized using a frame grabber. A calibration grid placed at the location of the mesh is used to correct for optical and geometrical distortions of the image. A stepper motor moves the electron gun in the radial direction so that a family of flux surfaces can be imaged.

FIG. 1(a) shows a set of flux surfaces that have been captured, digitized and corrected for distortion. There is no observable evidence of island structures inside the separatrix. A numerical calculation of the flux surfaces using a Biot-Savart code, inside the frame supporting the wire mesh, is shown in FIG. 1(b). A comparison of the experimental determination of the rotational transform to the calculated value is shown in FIG. 1(c). The agreement is good to within 1%.

3. Passing Particle Orbits and the Magnetic Field Spectrum

The deviation of a passing electron orbit from a magnetic surface can be used to determine the dominant $m \neq 0$ terms in the magnetic field spectrum. For particles launched along the field line such that the magnetic moment $\mu \sim 0$, the guiding center equations in the Boozer coordinates r, θ, ϕ are as follows [1],

$$B_0 r \frac{dr}{dt} = -\frac{M v_{\|}^2}{eB} \frac{dB}{dq}, \tag{2a}$$

$$\frac{dq}{dt} = \frac{\iota B v_{\|}}{g} + \frac{M v_{\|}^2}{eB} \frac{1}{B_0 r} \frac{dB}{dr}, \tag{2b}$$

$$\frac{df}{dt} = \frac{B v_{\|}}{g}. \tag{2c}$$

In the above equations, M is the particle mass, g is related to the poloidal current outside a flux surface and r is a flux surface variable given by $r = (\psi/\pi B_0)^{1/2}$ (ψ is the toroidal flux and B_0 is the field at the magnetic axis). Terms in the guiding center equations dependent on the toroidal current within a flux surface have been set to zero because of the curl-free field in the

vacuum configuration. The magnetic field spectrum, given by Eq. 1, explicitly enters the guiding center equations from the dB/dθ term in Eq. 2(a). Ignoring the term dependent on the radial derivative of the magnetic field on the right side of Eq. 2(b) (the effect of this term will be considered in the next section), and assuming that for small drifts off the flux surface the rotational transform and the spectral components of the field do not depend on the flux coordinate r, a simple expression for the particle orbit can be obtained,

$$r^2 = r_0^2 + \frac{2Mv_{\|}g}{eB_0^2}\sum b_{nm}\frac{m}{n-m\iota}\left[\cos(n\phi - m\theta) - a_{nm}\right]. \qquad (3)$$

The constants $a_{nm} = \cos(n\phi_0 - m\theta_0)$ ensure that when the particle is initialized at the Boozer angles ϕ_0 and θ_0, the radial coordinate r is equal to r_0, the home flux surface. In the expression above, we have also assumed that $B \sim B_0$. From Eq. 3 it can be seen that m = 0 spectral components do not contribute to the drift of a passing particle in the radial direction. However, for spectral components such that $n - m\iota \approx 0$, even small amplitude terms can have a large effect on the drift orbit.

4. Experimental Measurement of the Spectrum

The number of toroidal planes in which the fluorescent mesh can be located limits the number of spectral components that can be determined by this method. In this experiment we were constrained to placing the mesh inside 3 large Box Ports, spaced 90^0 apart where the field periods are joined together. The three port locations were 7^0, 83^0, and 173^0 from the electron gun. To observe the drift of a passing electron from a flux surface, the magnetic field was lowered to 90 gauss and the energy increased to 450 eV. FIG. 2 shows the orbit shift of the higher energy particle with respect to one at 50 eV. The contrast for the images shown has been enhanced in order to clearly illustrate the shift. The gun position was the same for all three locations, roughly the half-radius of the plasma on the inboard side of the torus.

To determine the magnetic field spectrum using Eq. 3, it is first necessary to transform the experimental data to Boozer coordinates. The Boozer toroidal angle $\phi = (1/g)\int Bdl$ was determined from a model numerical calculation to be within a few degrees of the standard cylindrical toroidal angle in the lab frame of reference. Therefore, the laboratory toroidal angle was used as the Boozer toroidal angle. The Boozer poloidal angle is then given by $\theta = \iota\phi$ for each successive pass of the electron beam, where $\iota(\psi)$ is experimentally determined. To obtain the flux surface variable r, the area enclosed by each flux surface was used instead of the toroidal flux. Four flux surfaces in the vicinity of the drift orbit and 13 points on each flux surface for each of the three toroidal locations were used to develop a map between the lab reference frame and the Boozer coordinates. A neural network [2] then generalized the mapping and transformed the coordinate system for the high-energy particles. To avoid overfitting, a testing data set verified whether the mapping was sufficiently general.

Once the high-energy orbits have been mapped into Boozer space, Eq. 3 was used to obtain a best fit of the magnetic spectral components to the data. At normal operating fields of 0.5-1.0 T for HSX, the earth's field is ignorable. However, for the very low magnetic field at which the data was obtained, the earth's magnetic field needs to be considered because it adds a small b_{11} component to the quasihelical spectrum. As seen from Figure 1c, since the transform varies from 1.06 to 1.12 in HSX, this mode is resonant with the transform and produces a relatively large perturbation of the beam orbit.

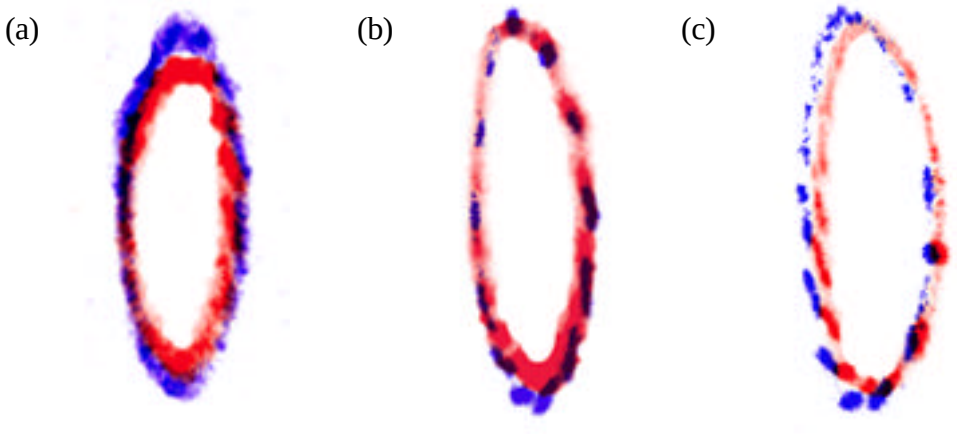

Figure 2. High energy (450 eV, red) and low energy (50eV, blue) electron orbits at (a) Box Port D, located 7^0 toroidally from electron gun (b) Box Port C (83^0) (c) Box Port B (173^0). The outboard side is to the right.

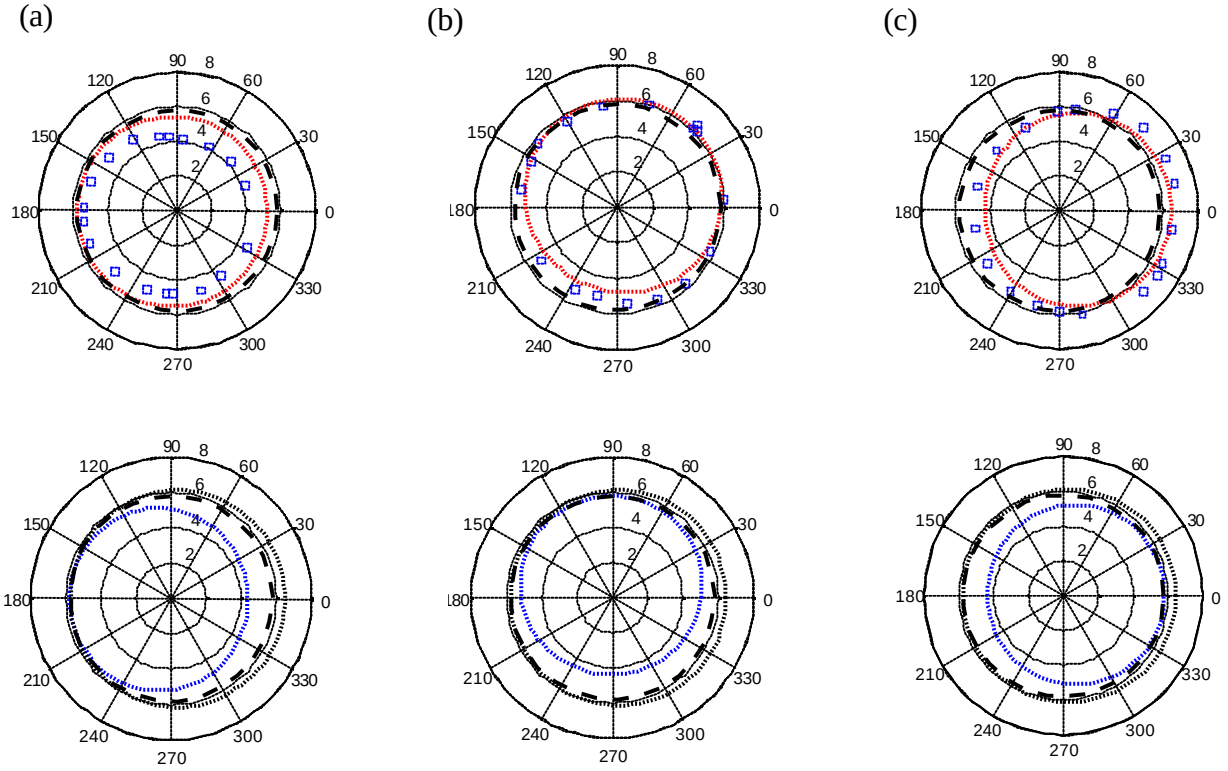

FIG. 3. Experimental data (blue squares) mapped from FIG. 2 into Boozer coordinates and the best fit (red) of Eq. (3). The starting flux surface of the electron beam is the black dashed line. Below each graph is the individual contribution of the b_{11} mode (blue) and the b_{41} (black) to the drift orbit. Shown are the orbits for (a) Box Port D (b) Box Port C (c) Box Port B. The outboard side is to the right.

FIG. 3 shows the Boozer transformation of the high-energy orbit as well as the best fit to the experimental data. Because of the symmetric placement of the fluorescent mesh, the contribution to the orbit from the b_{41} component of the spectrum is the same for all 3 cases. However, the b_{11} contribution rotates by 90^0 in going from one port to the other in the figure. At Box Port B, located almost 180^0 away from the electron gun, the deviation of the particle orbit on the outboard side is almost solely due to the b_{41} term, while on the inboard side it is

due to the b_{11} component. The best fit of the analytic expression to the data gives a value of b_{11} = 0.0023 and b_{41} = -0.051. Solving the coupled differential equations in Eq. 2, including the dB/dr that was neglected to derive Eq. 3, yields b_{11} = 0.0023 and b_{41} = -0.045. For this case it was assumed that the b_{41} term increased linearly with the flux coordinate r. The results are an underestimate of the spectral components because of the nonzero energy of the beam used to perform the Boozer coordinate mapping. Using Eq. 3 to solve for the home flux surface at zero energy (rather than 50 eV) yields b_{11} = 0.0034 and b_{41} = -0.077.

For comparison, we included a model earth's field [3] at the location of the laboratory into a code that calculates the Boozer spectrum, assuming an ideal coil representation for HSX. The calculation yielded the spectral amplitudes b_{11} = 0.003559 and b_{41} = -0.07262. The close agreement to the data does not reflect the errors in the measurements. The phase of the b_{11} mode from the calculation differed by approximately 45^0 from the experimental data.

5. Conclusion

The placement of the fluorescent mesh in 3 Box Ports spaced 90^0 apart does not allow for an unambiguous measurement of the toroidal curvature. For example, the b_{41} term is not distinguishable from a b_{01} or a b_{81} mode at these locations. However, the passing particle orbits shown in FIGS. 2 and 3 are not consistent with the negative sign of the toroidal curvature term (low field on the outboard side) that is present in other toroidal devices. Shown in FIG. 4 is the drift orbit of a passing particle in a magnetic field with only toroidal curvature (such as an ideal tokamak) with a magnitude equal to the b_{41} term shown in FIG. 3; ie. b_{01} = -0.051. Note in this case the deviation of the particle orbit on the outboard side would always be to the inside of the home flux surface. This can be contrasted to the data observed at Box Port B. For this case, the orbit on the outboard side is outside the flux surface. Note too that the deviation of the orbit due to the b_{41} term is on the order of 1/3 that due to the b_{01} component because of the $n - mi$ factor in Eq. 3. Within the constraints imposed by the experiment, this result is the first demonstration of the transport-optimized properties of the quasihelical stellarator.

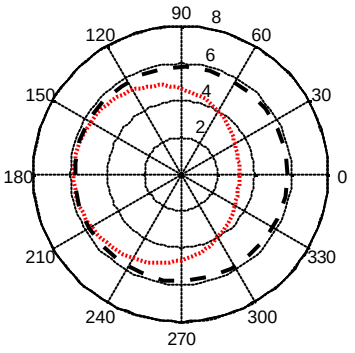

FIG. 4. Passing orbit of an electron in a magnetic field with only toroidal curvature. The outboard side is on the right.

Acknowledgement

This work is supported by US DoE under grant DE-FG02-93ER54222.

References

[1] Boozer, A.H., Phys. Fluids **23** (1980) 904.
[2] Neural Network Toolbox, distributed by The Math Works Inc., Natick, MA.
[3] Geomagix, written by John Quinn of the US Geological Survey, distributed by Interpex Limited of Golden, Colorado, USA., http://geomag.usgs.gov/Freeware/geomagix.htm.